Unpredictable behavior in the Duffing oscillator: Wada basins

Jacobo Aguirre, Miguel A.F. Sanjuán*

*Nonlinear Dynamics and Chaos Group, Departamento de Ciencias Experimentales e Ingeniería,
Universidad Rey Juan Carlos, Tulipán s/n, 28933 Móstoles, Madrid, Spain*

Abstract

This paper describes some numerical experiments giving evidence of Wada basin boundaries for the Duffing oscillator. We suggest some mechanisms by which this fractal property of the boundaries appears and discuss the difficulties that the Wada property presents for predicting the behavior of dynamical systems.
© 2002 Elsevier Science B.V. All rights reserved.

1. Introduction

When studying nonlinear dynamical systems, different global structures typically arise when one parameter is varied. One of the goals of nonlinear dynamics is the determination of how these global structures, such as strange attractors or other strange sets (basin boundaries, nonattracting chaotic sets, etc.), arise with the simple variation of a parameter of the system. A typical phenomenon in dynamical systems is the coexistence of attractors for a chosen set of parameters, which is responsible for the approach of different asymptotic states depending on the initial condition. In particular, when we have two attractors in the phase plane, the set of initial conditions that go to one of the attractors defines the attractor's basin of attraction. If there are two attractors, then there

are two basins, and consequently there is a curve that separates both basins, which is called the basin boundary. A point x belongs to the boundary, and is a boundary point, when there is an open set surrounding x which intersects both basins. Thus, the basin boundary is defined by the set of boundary points. The basin boundary is an invariant set, i.e., if x and its image belong to the basin boundary, then every subsequent image belongs to the boundary.

The basin boundary can be a smooth curve, but it also can be a fractal structure. We say that a basin boundary is fractal if it contains a transversal homoclinic point. A *transversal* homoclinic point q is a point of intersection where the stable and unstable manifolds associated to a hyperbolic fixed point p cross and are not tangent. This result was first encountered by Moon and Li [1]; it is related to the Melnikov theory [2], which is one of the few analytical methods used to ascertain the homoclinic bifurcations of a dynamical system. The Moon and Li

---

* Corresponding author.
E-mail address: msanjuan@escet.urjc.es (M.A.F. Sanjuán).

result proves that over a certain threshold value, homoclinic bifurcations occur, after which a transversal homoclinic point exists; this situation leads to chaos of the Smale-horseshoe type, and as a consequence the boundaries become fractal. In other words, the Moon and Li result implies that a transition occurs on the basin boundary from being smooth to fractal, when a parameter surpasses a critical value for which a transversal homoclinic point exist. Basin boundaries with this property are called fractal basin boundaries (for an excellent description of them, see Ref. [3]).

When three attractors coexist in phase space, a new phenomenon is possible, namely the *Wada property* [4–7]. The goal of the present work is to show that basin boundaries of the Duffing oscillator can have the Wada property. The Duffing oscillator is a well-known model of a nonlinear oscillator, with applications in many fields of applied sciences and engineering. In fact, it is viewed as a paradigm in nonlinear dynamics, and for this reason it has been studied by many authors (see for instance Ref. [8], and references therein). The Wada property was first introduced in the physics literature by Kennedy and Yorke [4]. This reference illustrates the nature of Wada basins and pays particular attention to the topological properties underlying them.

A basin boundary satisfies the Wada property if every open neighborhood of any point on the boundary has a nonempty intersection with at least three different basins. To possess the Wada property is stronger than to have fractal basin boundaries. In fact, if a dynamical system has the Wada property, then it must have fractal basin boundaries, but the converse is false. For the Wada property to hold, the system must have three or more coexisting attractors, but for a fractal basin boundary to exist, only two are needed.

Basin boundaries with the Wada property, like fractal basin boundaries in general, lead to *final state sensitivity* [3,9,10], i.e., serious problems in the prediction of the behavior of the dynamical system. The existence of Wada basin boundaries has been reported for both hamiltonian and dissipative systems. Some examples can be found in [11] in relation to a problem of a billiard system, in [12–14] in the context of chaotic advection of fluid flow, in [15] for a forced

predator–prey model in ecology and in [16] for the Hénon–Heiles hamiltonian system. Moreover, Wada basins have been found in an interesting and simple experiment in chaotic scattering by Sweet et al. [17].

Some computational algorithms to verify the Wada property for certain dynamical systems were introduced by Nusse and Yorke [5]. They are especially applicable to dissipative systems. Moreover, they introduce some new concepts, such as basin cells, which we will describe later in this paper, and give numerically verifiable conditions under which a dynamical system possesses the Wada property. We will use these computational tools to prove that the Duffing oscillator for a certain set of parameters has Wada basin boundaries.

In the next section, we explain the Wada property and argue that the Duffing oscillator possesses it. In spite of the literature on this problem, we believe that the consequences of Wada basins on predictability have not been sufficiently studied. For this reason, we have attempted to assess the unpredictable behavior arising from Wada basins. In Section 3, we show that Wada basins are an intermediate case between the partial predictability of fractal basins and the total unpredictability of riddled basins. Section 4 contains some concluding remarks.

2. The Wada property and the Duffing oscillator

The main focus of this section is to show strong evidence that the Duffing oscillator has the Wada property. To fix the ideas clearly, we say that a point x on a basin boundary is a Wada point if every open neighborhood of x has a nonempty intersection with at least three different basins. A basin boundary is a *Wada basin boundary* if all of its points are Wada points. In [5], it is shown that a basin is Wada if the unstable manifold of each of its accessible periodic orbits intersects at least three basins. (This result yields a practical computational tool for dissipative systems.) A point p on the boundary of a basin B is accessible from B if a curve can be drawn, starting in the interior of B, in such a way that p is the first point of intersection of the curve with the boundary of B (see Fig. 1 for a schematic explanation of this concept).
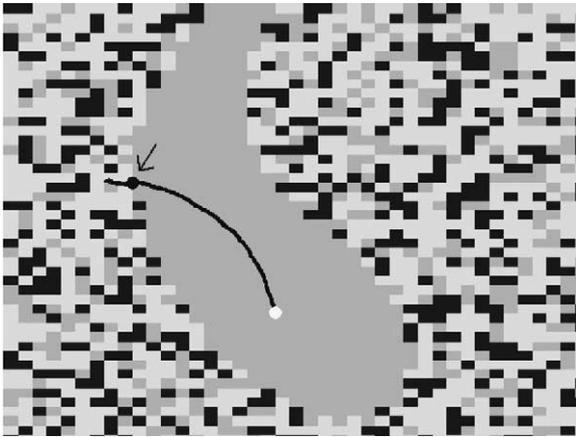
Fig. 1. The black point is accessible from the gray basin, because it is the first boundary point that a curve hits starting from the interior of the basin.

The Duffing oscillator may be understood as a model of the one-dimensional motion of a particle of unit mass in a double-well potential with dissipation and external periodic forcing. It can be written as

$$\ddot{x} + \delta\dot{x} - \alpha x + \beta x^3 = \gamma \cos \omega t. \tag{1}$$

The variable $x(t)$ is the position of the particle at time t and δ is the damping coefficient. The parameters γ and ω are the amplitude and frequency of the external perturbation. The following parameters have been fixed throughout the paper: $\delta = 0.15$ and $\alpha = \beta = \omega = 1$. We vary the parameter γ, i.e., the amplitude of the external perturbation. We have concentrated our study on the interval $0.24 \leq \gamma \leq 0.26$, where several attractors coexist.

The Poincaré time-2π map associated with Eq. (1) has two fixed-point attractors and a period-3 attractor for the parameter value $\gamma = 0.2445$. A plot of the periodic fixed points for the Poincaré time-2π map is shown in Fig. 2. To compute the fixed points we have used a simple Newton method with random initial conditions.

We call P_1R and P_1L the period-1 orbits located on the right and on left, respectively. We call P_3L, P_3C and P_3R the left, center and right points of the period-3 attractor, respectively. The period-1 attractors are located at $P_1R \approx (0.815, 0.242)$ and $P_1L \approx (-0.933, 0.299)$. The period-3 attractor is located at $P_3L \approx (-1.412, -0.137)$, $P_3C = (-0.354, -0.614)$,
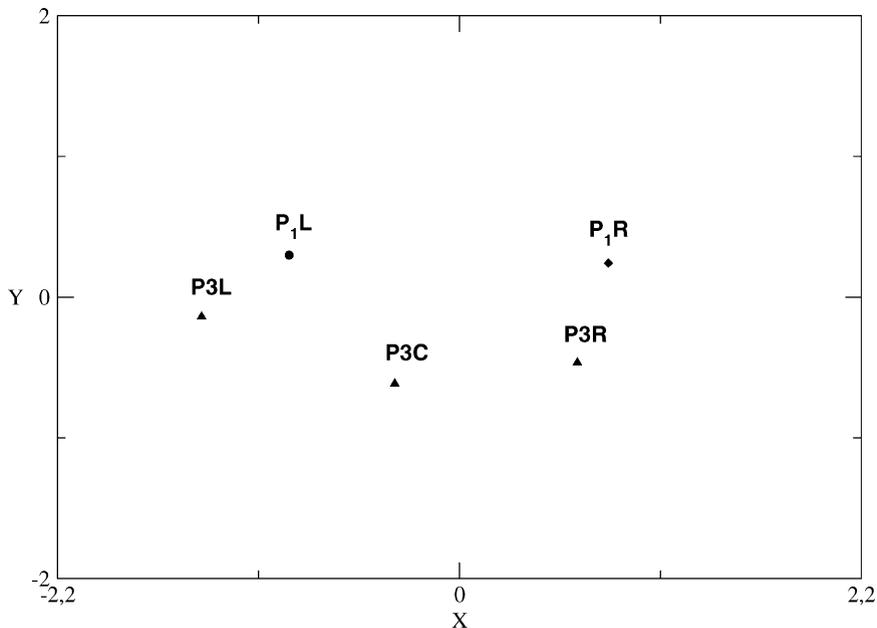

Fig. 2. This figure shows the position of the three coexisting attractors in the Poincaré 2π map associated to the Duffing oscillator. There is a period-1 attractor on the right (P_1R), a period-1 attractor on the left (P_1L) and a period-3 attractor (P_3L, P_3C and P_3R).
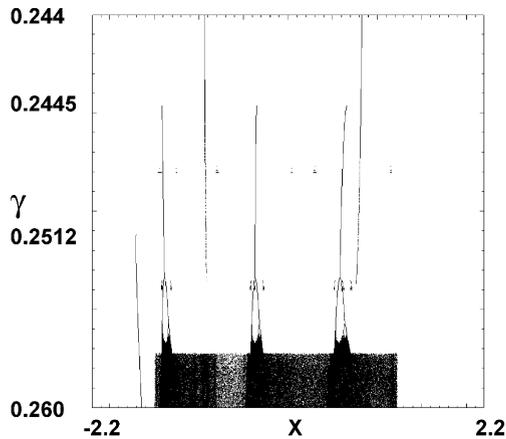
Fig. 3. A bifurcation diagram for many initial conditions taken randomly for the range of parameters γ ranging from 2.44 to 2.6. Note that there is an interval of γ values ranging from 0.2445 to 0.2512 for which three attractors coexist.

Fig. 4. The picture shows the basin of attraction diagram. A fine grid of 960×960 of initial points is considered and different colors are chosen according to which attractor an initial condition goes to. There are some regions where the likelihood of going to the attractor is bigger, but it is clearly observable that for most parts of the phase space the situation is very complicated.

and $P_3R = (0.645, -0.464)$. Additional evidence of the coexistence of these three attractors comes from Fig. 3, which shows the bifurcation diagram for many initial conditions taken randomly. It is interesting to note in Fig. 3 that the period-3 orbit arises from a saddle-node bifurcation at $\gamma = 0.2445$ and follows a typical period-doubling route to chaos as γ increases further. At $\gamma = 0.2512$, a new saddle-node bifurcation occurs, giving rise to a period-1 orbit.

All the numerical computations were made using a fourth-order Runge–Kutta integrator with a fixed time step of $2\pi/500$. Of central importance for this work is the computation of the basin diagram for this system. To numerically generate the basins of attraction, we selected a grid of 960×960 points, which were taken as initial conditions. Each initial condition was integrated until the corresponding trajectory approaches one of the attractors. The initial condition was then plotted in a color that corresponds to the attractor. Fig. 4 shows the numerically computed basin boundary. The calculations took several days on a Pentium PC. This simple fact may explain the complexity of the basin structure, since often the computation of a simpler basin is less time-consuming. We estimate that its uncertainty dimension [3] is $d = 1.98 \pm 0.01$ (for nonfractal basins, $d = 1$), which indicates a highly fractal structure. As we have three attractors, there are
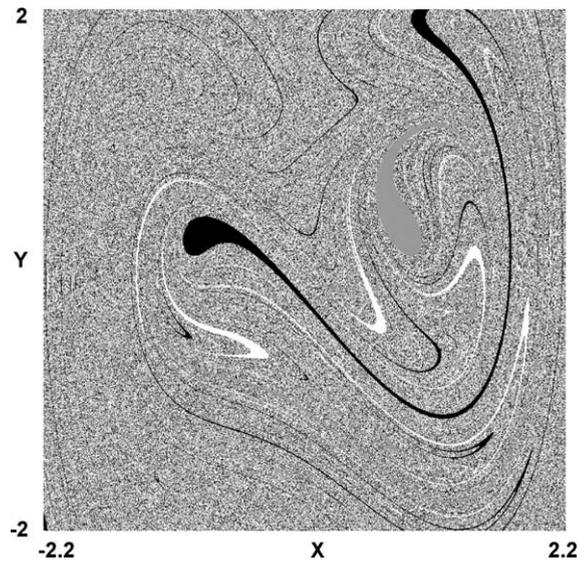
three different basins of attraction for this choice of parameters, which we have colored black, gray and white. One key question arises: is the black basin a Wada basin? If so, every boundary point of the black basin is also a boundary point of both the gray and the white basins. Before answering this basic question, we need to go first to some important concepts.

Given a dynamical system, a *trapping region* is a region in phase space from which points cannot escape. Once a trajectory enters a trapping region, it never leaves; thus a trapping region must contain an attractor (ω-limit set). This is known as the *lockout property* [18]. The notion of a *basin cell* [5–7,14] also plays a fundamental role. A basin cell is a trapping region whose boundary consists of pieces of stable and unstable manifolds of an accessible boundary periodic orbit (see Fig. 5 for a clarifying diagram).

All our discussion is based upon a theorem by Nusse and Yorke [5] that basically says: assume a basin with a basin cell. If there is a periodic orbit that generates a basin cell, and one of the branches of the orbit's unstable manifold passes through at least two other
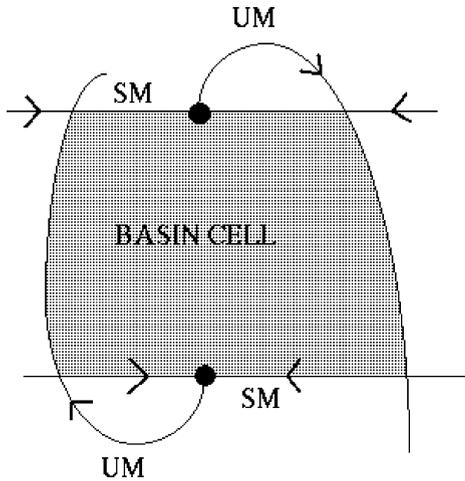
Fig. 5. A basin cell is a trapping region formed by *n*-pieces of the stable and unstable manifolds of an accessible boundary *n*-periodic orbit (in the present diagram, a period-2 orbit).

basins of attraction, then the basin has the Wada property. Another important result appears in [19], which has to do with a saddle-node bifurcation that occurs on fractal basin boundaries.

What is observed here is a clear example of the Wada bifurcation criterion stated in [19]. We have observed that at $\gamma = 0.2445$, a saddle-node bifurcation gives rise to a period-3 orbit. For values of γ that are slightly smaller than 0.2445, there are two fixed-point attractors, and the basin boundary is fractal. This phenomenon is an interesting example of a transition between a fractal and Wada basin boundary when a system parameter is varied. More precisely, a saddle-node bifurcation creates a new coexisting attractor, so the system passes from two to three attractors, which is a necessary condition for Wada basins to exist. (A much more interesting question would be to study this transition from fractal to Wada basin boundaries in a situation in which three or more basins coexist before and after the transition.)

The previous observation of the birth of an orbit via a saddle-node bifurcation can be also proved by the Moon and Li criterion [1], which applies the Melnikov theory for the appearance of a homoclinic point. At $\gamma = 0.2512$, a new saddle-node bifurcation occurs, giving rise to a period-1 orbit, whose basin boundary

is exactly the stable manifold of the saddle, which is a smooth curve of dimension 1. At $\gamma = 0.258$, an interior crisis occurs, and a period-1 orbit coexists with this enlarged chaotic attractor, which is the development of a period-doubling route to chaos from the period-3 orbit born at $\gamma = 0.2445$. So, for most parameter values in the region $0.2445 \leq \gamma \leq 0.2512$, a period-3 orbit coexists with two period-1 orbits, so there are three basins of attraction. The value we have chosen for the computation of the basin of attraction diagram is $\gamma = 0.2445$, which belongs to this interval, and we believe that for this range of γ values, the system has the Wada property. (Moreover, as mentioned in [19], indeterminate bifurcations in the sense of Thompson may occur as γ decreases past 0.2445. When one basin disappears, we cannot determine to which of the two remaining basins the orbit goes.)

The *Wada interval W_γ* associated with the parameter γ is an open set of parameter values γ for which the system has the Wada property. In other words, we say that $\gamma_0 \in W_\gamma$ if, for the parameter γ_0, the system possesses the Wada property. In our case, the Wada interval W_γ is approximately (0.2445, 0.2512). For every value of γ inside this interval, every boundary point is a Wada point and consequently belongs to the basin boundary of the three attractors.

We have carried out computations of the Lyapunov exponents for this Wada interval and they are strictly negative, showing that there are no chaotic orbits. Since this region is very close to an interior crisis, there is a nonattracting chaotic set, which can be computed using the PIM-triple method [20]. The chaotic saddle for this parameter set is shown in Fig. 6. It is an invariant set composed of the intersection of the stable and unstable manifolds of a saddle orbit in phase space, and it is responsible for the chaotic transients that are present in the dynamics of the oscillator.

There are several ways to check whether a basin B has the Wada property [16]. In our case, we have decided to show that the Duffing oscillator satisfies the conditions of Theorem 2 in [5], which is a useful numerical criterion for dissipative systems, described next. First, we must find an unstable periodic orbit P, accessible from basin B, that generates a basin cell. Secondly, the unstable manifold of P must intersect
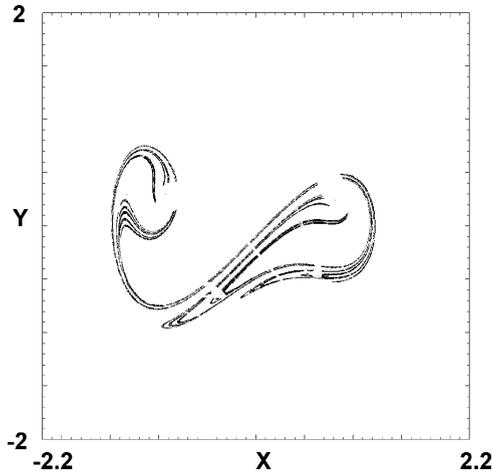
Fig. 6. A chaotic saddle corresponding to the situation for which the strong fractalization of phase space appears in the figure. The chaotic saddle is responsible for the chaotic transients that are present in the system.

all basins, and finally, it is necessary to repeat this strategy for each basin to confirm that all basins indeed have the Wada property.

Every basin in our system has an associated basin cell. A picture with each corresponding basin cell is shown in Fig. 7 for the gray basin, Fig. 8 for the black
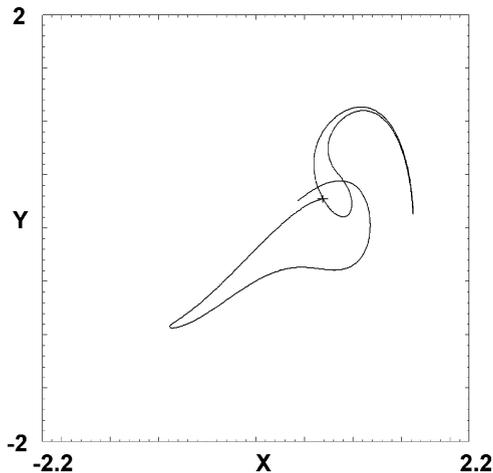

Fig. 7. This figure shows the basin cell B_3R, which encloses the P_1R attractor and is generated by the saddle $S_1L \approx (0.689, 0.276)$. It is important to compare it with the Fig. 4 of the basin diagram and observe that the branch of the unstable manifold intersects the three basins of attraction, what gives evidence that this basin is Wada.

Fig. 8. This figure shows the basin cell B_1L, which encloses the P_1L attractor and is generated by the saddle $S_1L \approx (-0.895, 0.407)$. It is important to compare it with the Fig. 4 of the basin diagram and observe that the branch of the unstable manifold intersects the three basins of attraction, what gives evidence that this basin is Wada.
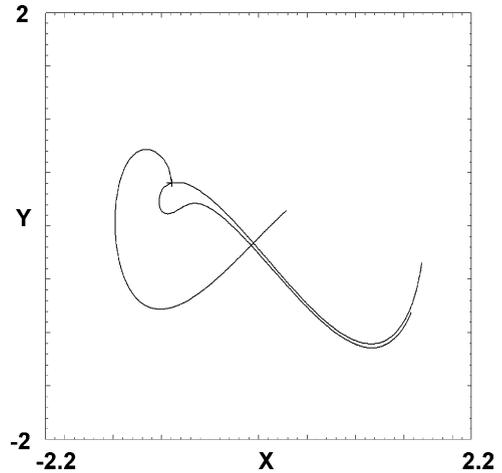
basin, and Fig. 9 for the white basin. The structure of the basin cells is as follows. Each basin cell is generated by an accessible periodic boundary point. We have three basin cells. The basin cell B_3R, which encloses the period-1 attractor P_1R, is generated by the saddle point $S_1R \approx (0.689, 0.276)$ and is shown in Fig. 7. The basin cell B_1L, which encloses the period-1 attractor P_1L, is generated by the saddle point $S_1L \approx (-0.895, 0.407)$ and is shown in Fig. 8. The basin cell associated with the period-3 attractor is formed by three disconnected basin cells, which we call B_3L (shown in Fig. 9(a)), B_3C (shown in Fig. 9(b)) and B_3R (shown in Fig. 9(c)). Each one is generated by the saddles $S_3L \approx (-1.411, -0.032)$, $S_3C \approx (-0.339, -0.613)$, and $S_3R \approx (0.685, -0.459)$. All the accessible boundary points have been calculated using the ABST algorithm with Dynamics [21]. (The ABST method is explained thoroughly in [22].) In fact, the accessible unstable saddle points determine the structure of the boundary. We have plotted in Figs. 7–9 the unstable manifold of each accessible unstable periodic orbit. By comparing these pictures with Fig. 4, it is evident that the unstable manifolds cross all three basins. These computations provide clear evidence that, for the range of parameters analyzed
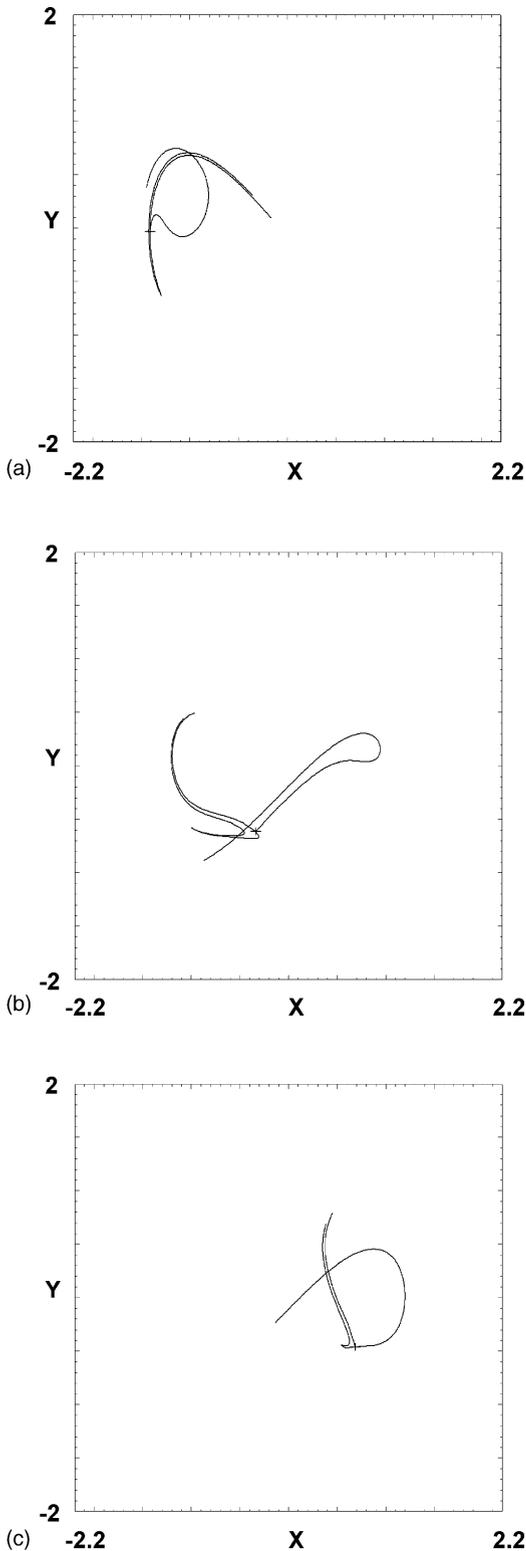
in this paper, the attractor basins for the Duffing oscillator have the Wada property.

3. Unpredictability

One of the main consequences of Wada basins is related to the difficulty of predicting to which attractor a given initial condition might go. This is very important, since we are used to the naive idea of classical determinism, where once the initial condition is fixed, automatically we know the evolution of the orbit. While every initial condition has a unique orbit in the Duffing oscillator, the phase space is so intertwined that serious difficulties in prediction arise if there are small uncertainties in fixing the initial condition.

If the initial condition belongs to a basin cell, then it is situated in the interior of a trapping region. Consequently, even if there is a slight uncertainty in the precise location of the initial condition, we have high certainty in predicting the attractor to which the initial condition goes: it is the attractor that exists inside the basin cell. Nevertheless, as is clearly seen from our basin diagram in Fig. 4, this is not the situation for most initial conditions in phase space. In particular, suppose we choose the initial condition $(x(t_0), \dot{x}(t_0)) = (0, 0)$. For this choice, the trajectory tends to a period-3 orbit in phase space, which is one of the three coexisting attractors. When we modify slightly this initial condition to, say $(0.004, 0)$ the trajectory tends to the period-1 orbit on the right well. However, the trajectory starting from the initial condition $(-0.02, 0)$ tends to the period-1 attractor in the left well, as does the trajectory from the initial condition $(0.012, 0)$. This simple numerical experiment illustrates the lack of practical predictability in this simple situation where three periodic attractors

Fig. 9. The figure shows the three disconnected basin cells corresponding to the period-3 attractor: (a) basin cell B_3L generated by the saddle $S_3L \approx (-1.411, -0.032)$; (b) basin cell B_3C generated by the saddle $S_3C \approx (-0.339, -0.613)$; (c) basin cell B_3R generated by the saddle $S_3R \approx (0.685, -0.459)$. As in the previous cases, note that the branches of the unstable manifolds intersects the three basins, implying that B_3 or the white basin is Wada.

coexist in phase space. From an experimental point of view, fixing an initial condition with such precision may not be possible; consequently, there is a serious problem in prediction. Few authors have focused on this issue, and a thorough discussion on it is one of the goals of the paper. We have carried out several numerical experiments to gain a better understanding of the unpredictability of the Duffing oscillator for this special choice of parameters.

The first experiment was conducted as follows. Consider a thin horizontal strip for which $x \in (-2.2, 2.2)$. The height is chosen in such a way that a great portion of the basin cells of the period-1 orbits are inside the strip, for instance, $v \in (0.1, 0.2)$. We cut the strip vertically into 200 narrow slices, each of whose dimensions is then 0.022×0.1. A grid of 2000 initial conditions is taken inside each slice, and for each initial condition, the system is integrated until

an attractor is reached. We evaluate the probability of reaching each periodic attractor for all the slices by calculating the percentage of orbits that leads to each one. We have plotted this probability depending on the positions of the x coordinate of the center of each slice. The results of the experiment are shown in Fig. 10. The original horizontal strip intersects both fractal and nonfractal (smooth) regions. When one of the smaller slices is contained entirely in a nonfractal region, the probability that the initial conditions contained in it go to one of the attractors is 100%, and the probability of going to one of the other two attractors is zero. Hence, there is no problem in trying to predict the future behavior of the system from inside the slice. However, if a portion of one of the slices includes a fractal region, then the probabilities are different, and the system is less predictable than in the last case. Finally, if a slice is in a fractal region, then the
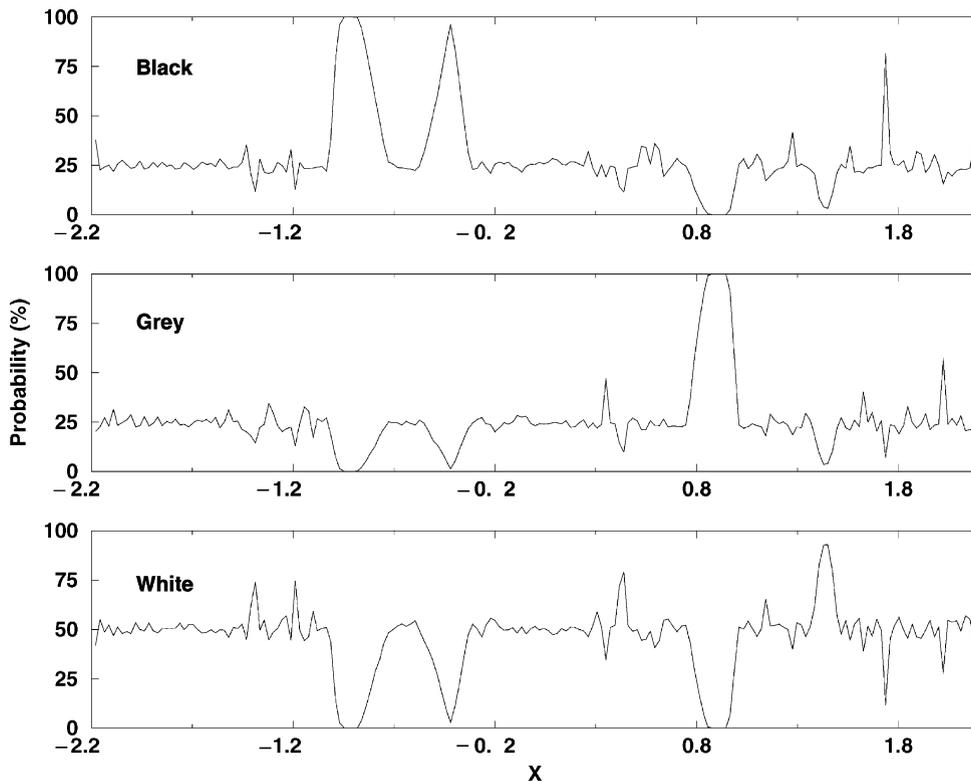

Fig. 10. The figure shows the probability versus the coordinate x for a small rectangle around zero. The upper panel shows the probability for the attractor in the black basin. The central panel for the attractor in the gray basin and the lower panel for the attractor in the white basin.

probabilities tend to limiting values of 25% for the black and gray attractors and 50% for the white attractor.

In this situation, only a probabilistic study is possible. Fig. 10 shows the three regimes clearly. We can suppose that the size of the slice is the precision of our experiment, and in fact these three different regimes of predictability arise independently of the size of the slice. Obviously, the smaller is the slice, the more regions of total determinism (probability 100% for approaching one of the attractors) will appear, but there will always be regions with the other two behaviors. The reason is that this mixture of fractal and non-fractal regions in the phase space of initial conditions exists at all scales. We repeated the experiment by considering a small rectangle of size $-0.1 \leq x \leq 0.1$ and $-0.1 \leq y \leq 0.1$, with similar results. The main point here is that, for a given precision in the mea-

surement of the initial conditions, the final state of the system can be described only in probabilistic terms, even though the underlying dynamical process is deterministic.

In another numerical experiment, we chose 100 initial conditions along the vertical line segment from $(0, -2)$ to $(0, 2)$. Each initial condition was integrated until the trajectory reached a periodic attractor. The result of this experiment is shown in Fig. 11(a), where B indicates a point whose trajectory approached the black attractor, G the gray attractor, and W the white attractor. An erratic pattern results, which gives an idea of the unpredictability of the system. Next, we considered 100 initial conditions in the vertical segment from $(0, -0.02)$ to $(0, 0.02)$; the result is shown in Fig. 11(b). We repeated the process for the segment $(0, -0.0002)$ to $(0, 0.0002)$ (see Fig. 11(c)). Finally, Fig. 11(d) shows the results for a segment that is 100
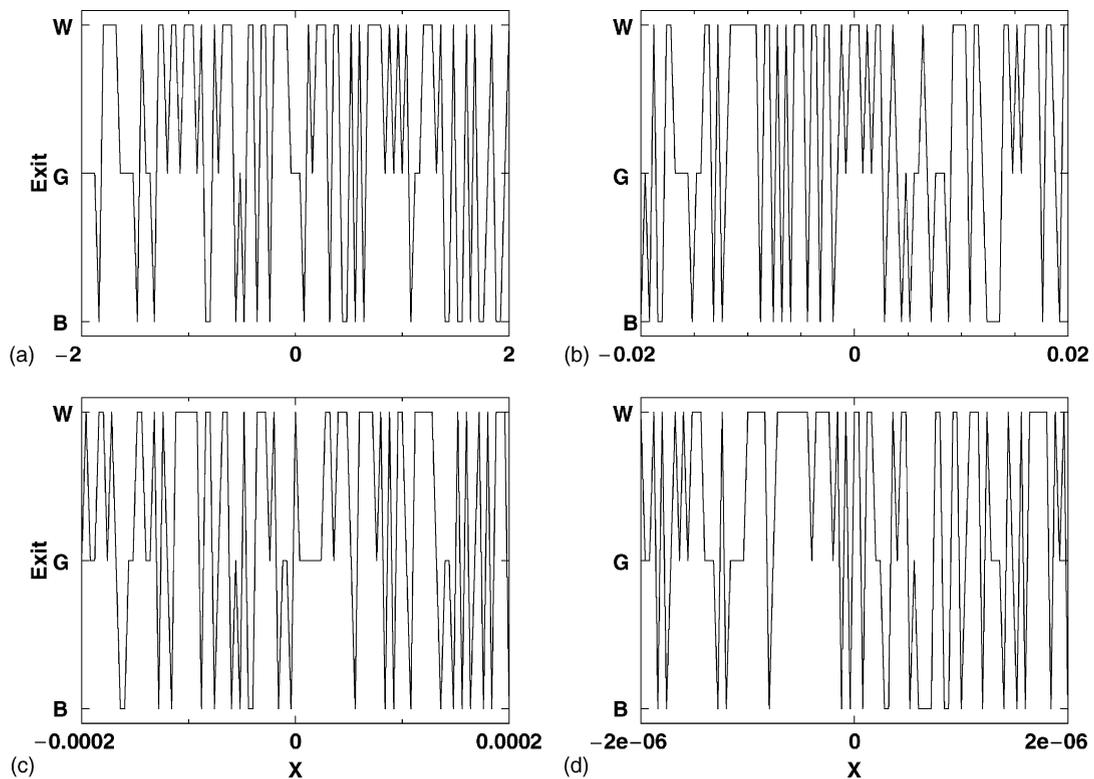

Fig. 11. The figures show the result of plotting to which attractor an initial condition goes versus different ranges of the y coordinate: (a) 100 points out of the whole interval ranging from -2 to 2 is chosen; (b) 100 points out of the whole interval ranging from -0.02 to 0.02 is chosen; (c) 100 points out of the whole interval ranging from -0.0002 to 0.0002 is chosen; (d) 100 points out of the whole interval ranging from -2×10^{-6} to 2×10^{-6} is chosen.

times smaller still. All figures show that the structures repeat themselves at each scale and suggest that the unpredictability occurs at fine scales.

We can use symbolic dynamics to show this peculiar, unpredictable behavior based on the three symbols B, G and W. For the case shown in Fig. 11(a) we have

```
GGGGBWWWWGGGGBWGGBWWGWWGWWWGWBBWGWW
   WBGBWWBWWBWWWWGGGBWGWWWBWBBBWBWBW
   WWWGWGWGWBGGWWWGWBBWBBWBWBBGWBBGW.
```

A similar situation occurs for Fig. 11(b):

```
BGBWBBWWGGGGBGGWWBWBGWWWWWWWBWWBWBW
   BWWWBWWBWWBGWGWWWGWGWWBGWGBGBGGWG
   BWWWGWWWWBWWGBBBBWWGWGWWWWBWWGBWW.
```

For the situation described in Fig. 11(c), we have

```
GWGGWWGWGBBGGWWGGWBWGBWWWWWWBWWBGWW
   BGBWBBWWWGWBGGBWGGGGGGGWWGWWWGBWWWW
   GWBWBWWGBWWWWWGWGGBWBWBGWBWBWWWB
```

and for Fig. 11(d) we have

```
WGGWBWBGWGWGWWWGGGBWBGGGGWWWWWBGWWW
   WWWWWGWWWWGWBWBWWBWWGGBBWGWWBGBBB
   BWWBBWWBGWWWBWGGGBWGBWBWWWWWBWGWB.
```

As we can observe from these series of symbols, there are always open intervals where the same symbol is repeated. In other words, as can be inferred from observation of the basin diagram in Fig. 4, we can always find open sets of initial conditions that are attracted to one particular attractor. The extent of final state sensitivity for the Wada basins here is not as extreme as for riddled basins [23]. (An interesting discussion related to predictability in the presence of riddled basins is found in [24].)

Another interesting topic would be to analyze the role of small noise in the dynamics on the basin structures that appear in this problem. In principle, there are arguments showing that, for small noise, this basin structures persists [18], although it is clear that for large enough noise levels, all is destroyed. Nevertheless, for the complicated structures of the basins observed in Fig. 4, it seems clear that introducing even small amounts of noise in the dynamics would complicate even more the question of prediction.

4. Conclusions

We have given numerical evidence that the Duffing oscillator possesses the Wada property, and hence that it has Wada basin boundaries. We have found here that Wada basins occur in a parameter region after a saddle-node bifurcation leads to three coexisting attractors, one of which is a period-3 orbit. We have shown that there is a transition from fractal basin boundaries to Wada basin boundaries when the saddle-node bifurcation gives rise to a new attractor, but the question of whether that transition is possible when three attractors coexist remains open. One of the more interesting consequences of the Wada property for the Duffing oscillator, namely the difficulties in predicting to which attractor an initial condition goes, is discussed. The fractal structure of the phase space, due to the complicated nature of the boundary basins, has important implications for determining the final output of the system for a certain initial condition; a probabilistic approach is needed to predict the final state. Finally, we have shown that having Wada basin boundaries represents an intermediate situation between the case of having fractal basin boundaries and the more complex situation of riddled basins, where all deterministic prediction is lost.

Acknowledgements

References

[1] F.C. Moon, G.-X. Li, Fractal basin boundaries and homoclinic orbits for periodic motions in a two-well potential, Phys. Rev. Lett. 55 (1985) 1439–1442.

[2] S. Wiggins, Introduction to Applied Nonlinear Dynamical Systems and Chaos, Springer, New York, 1990.

[3] S.W. Mcdonald, C. Grebogi, E. Ott, J.A. Yorke, Fractal basin boundaries, Physica D 17 (1985) 125–153.

[4] J. Kennedy, J.A. Yorke, Basins of Wada, Physica D 17 (1991) 75–86.

[5] H.E. Nusse, J.A. Yorke, Wada basin boundaries and basin cells, Physica D 90 (1996) 242–261.

[6] H.E. Nusse, J.A. Yorke, Basins of attraction, Wada basin boundaries and basin cells, Science 271 (1996) 1376–1380.

[7] K. Alligood, T. Sauer, J.A. Yorke, Chaos: An Introduction to Dynamical Systems, 3rd Edition, Springer, New York, 2000.

[8] L. Virgin, Introduction to Experimental Nonlinear Dynamics, Cambridge University Press, Cambridge, 2000.

[9] C. Grebogi, E. Kostelich, E. Ott, J.A. Yorke, Multi-dimensioned intertwined basin boundaries: basin structure of the kicked doubled rotor, Physica D 25 (1987) 347–360.

[10] E. Ott, Chaos in Dynamical Systems, Cambridge University Press, Cambridge, 1993.

[11] L. Poon, J. Campos, E. Ott, C. Grebogi, Wada basin boundaries in chaotic scattering, Int. J. Bifurcat. Chaos 6 (1996) 251–265.

[12] Z. Toroczkai, G. Karoly, A. Pentek, T. Tel, C. Grebogi, J.A. Yorke, Wada boundaries in open hydrodynamical flows, Physica A 239 (1997) 235–243.

[13] A. Witt, R. Braun, F. Feudel, C. Grebogi, J. Kurths, Tracer dynamics in a flow of driven vortices, Phys. Rev. E 59 (1999) 1605–1614.

[14] H.E. Nusse, J.A. Yorke, Fractal basin boundaries generated by basin cells and the geometry of mixing chaotic flows, Phys. Rev. Lett. 75 (2000) 2482–2485.

[15] J. Vandermeer, L. Stone, B. Blasius, Categories of chaos and fractal basin boundaries in forced predator–prey models, Solitons Fractals 12 (2001) 265–276.

[16] J. Aguirre, J.C. Vallejo, M.A.F. Sanjuán, Wada basins and chaotic invariant sets in the Hènon–Heiles system, Phys. Rev. E 64 (2001) 066208.

[17] D. Sweet, E. Ott, J.A. Yorke, Escaping chaotic scattering, Nature 399 (1999) 315.

[18] M.A.F. Sanjuán, J. Kennedy, C. Grebogi, J.A. Yorke, Indecomposable continua in dynamical systems with noise: fluid past an array of cylinders, Chaos 7 (1997) 125–138.

[19] H.E. Nusse, E. Ott, J.A. Yorke, Saddle-node bifurcations on fractal basin boundaries, Phys. Rev. Lett. 75 (1995) 2482–2485.

[20] H.E. Nusse, J.A. Yorke, A procedure for finding numerical trajectories on chaotic saddles, Physica D 36 (1989) 137.

[21] H.E. Nusse, J.A. Yorke, Dynamics: Numerical Explorations, 2nd Edition, Springer, New York, 1997.

[22] H.E. Nusse, J.A. Yorke, A numerical procedure for finding accessible trajectories on basin boundaries, Nonlinearity 4 (1991) 1183–1212.

[23] J.C. Alexander, J.A. Yorke, Z. You, I. Kan, Riddled basins, Int. J. Bifurcat. Chaos 2 (1992) 795–813.

[24] J. Sommerer, The end of classical determinism, Johns Hopkins APL Tech. Dig. 16 (4) (1995) 333–347.